99-123

СООБЩЕНИЯ
ОБЪЕДИНЕННОГО
ИНСТИТУТА
ЯДЕРНЫХ
ИССЛЕДОВАНИЙ

Дубна

99-123

E13-99-123

V.P.Ladygin*

ANALYZING POWER OF *pp*- AND *np*-ELASTIC SCATTERING AT MOMENTA BETWEEN 2000 AND 6000 MeV/c AND POLARIMETRY AT LHE

*E-mail address: ladygin@sunhe.jinr.ru

1999

1 Introduction

Many experiments in intermediate and high energy physics require the use of polarized beams. The knowledge of beam polarization with a good accuracy is very important for such a kind of experiments. The traditional method of measuring the nucleon beam polarization at high energies is to analyze the asymmetry of proton-proton elastic scattering [1, 2]. This reaction is worth-while for this purpose because of a large cross section and analyzing power. To date, a considerable amount of nucleon- nucleon data with small errors at intermediate energies has been accumulated [3, 4]. This allows one to measure beam polarization with a good accuracy and to have a permanent control over the polarization during the experiment. But data are still scarce at energies higher than the maximum energy of SATURNE at Saclay for *pp*- and a half of that for *np*- elastic scattering. Therefore, to have an opportunity for measuring the beam polarization over the full range of energies provided with the accelerator, it is necessary to extrapolate the available data on analyzing power. As a result of such a procedure, there arises the problem of systematic error due to different parametrizations.

The aim of this paper is to describe the method of measuring the vector admixture of a polarized deuteron beam and hence the proton and neutron polarization inside the deuteron at the Synchrophasotron and the Nuclotron of the Laboratory of High Energies, JINR and to evaluate a possible systematic error of this method over the momentum domain between 2000 and 6000 MeV/c per nucleon.

2 On-line beam polarimeter

The polarimeter used to measure the vector admixture of the deuteron beam polarization is installed at focus F4 of the beam line VP1 at the Laboratory of High Energies, JINR. The main principle of the polarimeter is based on the measurement of the left-right asymmetry of *pp*- quasi-elastic scattering by detecting scattered and recoil particles in coincidence. The polarimeter consists of 2 arms installed at the angles corresponding to *pp*- elastic scattering kinematics. Signals from eight scintillation counters (four for each arm and two for scattered and recoil protons, respectively) define left and right scattering events. The solid angle of this polarimeter is $\Delta\Omega = 7 \cdot 10^{-4}$. More details are given in ref.[5].

The numbers of events scattered on the left and right are related to the beam polarization and the analyzing power as follows [6]:

$$N_L^{\pm} = N_L^0(1 + P^{\pm} \cdot A) \tag{1}$$
$$N_R^{\pm} = N_R^0(1 - P^{\pm} \cdot A), \tag{2}$$

where $N_L^{\pm,0}$ and $N_R^{\pm,0}$ are the corresponding counts of the left and right scattering events for the "$+$", "$-$" and "0" states of polarization; $P^{\pm}$ are the values of beam polarization for the states "$+$" and "$-$"; A is the analyzing power of *pp*- elastic scattering.

Hence, the values of beam polarization can be easily obtained from asymmetries taking into account a false asymmetry, which is evaluated using an unpolarized beam (state "0"):

$$p^{\pm} = \frac{1}{A}\frac{N_L^{\pm}/N_R^{\pm} - N_L^0/N_R^0}{N_L^{\pm}/N_R^{\pm} + N_L^0/N_R^0} \quad (3)$$

The main feature of the polarimeter installed at LHE is that it measures the vector polarization of a **deuteron** beam provided with the ion source POLARIS [7]. Assuming that the analyzing power of the quasi-free proton scattering in the deuteron is the same as for free protons, one can obtain the value of deuteron beam polarization which is equal to the proton and neutron polarizations.

This polarimeter was successfully used in the experiment on the measurement of the $\Delta\sigma_L$ of *np-* scattering [8]. It was also used to control the vector admixture of the tensor polarized deuteron beam [7] in the experiment on the measurement of the tensor analyzing power A_{yy} in deuteron inclusive breakup at 9 GeV/c [9, 10]. Fig.1 demonstrates the stability of asymmetries during the latter experiment. The open and full symbols represent the values of asymmetries $A^{\pm}$ obtained during the control measurements of the polarization and data taking, respectively. The averaged values of asymmetries obtained during the control measurements are 0.033 ± 0.004 and 0.035 ± 0.004 for the "+" and "-" polarization states, respectively. The corresponding averaged values of asymmetries obtained during data taking are 0.029 ± 0.004 and 0.031 ± 0.004. Both results are in good agreement [10].

The values of beam polarization obtained from this polarimeter were comparable to the values given by the 2-arm polarimeter ALPHA [11] based on *dp-* elastic scattering at 3 GeV/c. One of the possible reasons of a small discrepancy between the values of polarization from 2 polarimeters can be due to the precision of the *dp-* and *pp-* data on the analyzing powers. The investigation of possible systematic errors due to different parametrizations of *pp-* elastic scattering data over the energy range of the LHE Accelerator Complex is presented below.

3 Parametrization of the *pp-* elastic scattering analyzing power

The high momentum data (1.45 - 45 GeV/c) on the analyzing power A were fitted with the expression [1]

$$A(P_{lab}, t) = a \cdot \sqrt{-t} \cdot (1 + b \cdot t + c \cdot t^2), \quad (4)$$

where t is the 4-momentum; a,b and c are the constants depending on the laboratory momentum of the proton beam, P_{lab}. They are defined as follows:

$$\begin{aligned} a &= (D + E + E \cdot P_{lab} + F \cdot P_{lab}^2)/P_{lab} \\ b &= G + H \cdot log(P_{lab}) + J \cdot log(P_{lab})^2 \\ c &= K + L \cdot log(P_{lab}) \end{aligned} \quad (5)$$

Here the coefficients $D - L$ are the constants.

This fit performed for $|t| \leq 0.7$ (GeV/c)^2 gave a χ^2 of 4.59 per degree of freedom. A large value of χ^2 is due to large systematic errors of the used data for the fit. The authors also mention that the high precision *pp-* data at $-t \leq 0.2$ GeV/c^2 in small steps between 1.5 and 6 GeV/c would be important because the available data seem to have sizeable normalization problems and systematic errors.

In the last few years, a large body of data on different polarization observables for *pp-* elastic scattering has been accumulated up to the maximum energy of SATURNE. This allowed one to carry out a partial wave analysis up to a 2.5 GeV kinetic energy ($\sim$ 3.3 GeV/c of the laboratory momentum) [4]. Therefore, one can use the results on the analyzing power from fit [4] over this range. However, polarization data are still scarce at higher energies , and the phenomenological parametrization of the analyzing power as a function of initial energy (or momentum) and scattering angle (or 4-momentum) is very desirable.

We start with parametrization using analytic functions (4-5). All the data from review [3] at initial momenta between 2 and 6 GeV/c, namely [12]-[28], are included in the fit. The data base for this energy range is practically the same as that used for the fit performed in ref.[1]. However, the range of 4-momentum for the fit is twice as large as that in ref.[1] ($|t| \leq 1.5$ (GeV/c)^2). The restriction of the initial momentum domain must improve the quality of the fit because the data out of this range with large systematic errors do not affect the parameters. No relative normalization of the data from different experiments is done. The recent data obtained up to 3.5 GeV/c at Saclay are not included.

The results of the fit at four initial proton momenta (2.25, 3.0, 4.5 and 6.0 GeV/c) are presented in Fig.2. The solid lines are the fit of the data a the momentum domain of 2-6 GeV/c. The total number of data points is 488. This fit gives a χ^2 of 2.95 per degree of freedom to be compared with 4.59 [1]. The dashed lines represent the results of the fit (4)-(5) over an initial momentum range of 2-5.2 GeV/c (χ^2/n = 3.41). The dotted lines are the results of the fit for initial momenta between 2 and 2.5, 2.5 and 3.5, 3.5 and 5.2, 5.2 and 6.0 GeV/c, respectively. The optimum values for the 8-parameter fit (4)-(5) of the *pp-* elastic scattering data are presented in Table 1. The dash-dotted lines are the results of parametrization from ref.[1]. One can see that the results at small values of $|t|$ only weakly depends on the used parametrization. However, the results differ significantly at large $|t|$. Note that χ^2/n obtained for the data at momenta larger than 3.5 GeV/c is twice as small as that for all the data between 2.0 and 6.0 GeV/c. Therefore, using parametrizations over a momentum range of 3.5- 5.2 and 5.2-6.0 is more convenient to estimate the analyzing power in this momentum domain.

The parametrization of the analyzing power as a function of scattering angle and momentum is usually useful for a quick estimation of counting rates in experiments calling for a polarimeter.

The angular dependence of the analyzing power is fitted by the function as in ref.[29]. This analytical parametrization of the analyzing power depends on scattering angle, θ, and laboratory momentum, P_{lab}, as follows:

$$A(P_{lab},\theta) = a \cdot x^r \cdot e^{-b\cdot x} + c \cdot x^s \cdot e^{-d\cdot x} \tag{6}$$

with $x = P_{lab} \cdot sin(\theta)$, where P_{lab} is the proton momentum in GeV/c. The six quantities a, b, c, d, r and s are the functions of laboratory momentum:

$$\begin{aligned} a &= a_0 + a_1 \cdot P' + a_2 \cdot P'^2, \\ b &= b_0 + b_1 \cdot P' + b_2 \cdot P'^2, \\ c &= c_0 + c_1 \cdot P' + c_2 \cdot P'^2, \\ d &= d_0 + d_1 \cdot P' + d_2 \cdot P'^2, \\ r &= r_0, \\ s &= s_0, \end{aligned} \tag{7}$$

where $P' = P_{lab} - P_0$. Momentum P_0 given in GeV/c is chosen to be approximately in the center of the parametrization domain.

The results of the fit (6-7) at four initial momenta of protons are presented in Fig.3. The solid lines are the fit of the data for a momentum domain of 2-6 GeV/c ($P_0 = 4.0$ GeV/c). The data [3] included in the fit are taken in an angular domain of up to 30° in the lab. (528 points). This fit gives a χ^2/n of 2.94. The fit over a restricted momentum domain of 2-5.2 GeV/c ($P_0 = 4.0$ GeV/c) with the total number of points 381 gives a χ^2/n of 3.17. The results of this fit are given by the dotted lines. If we exclude the points with momenta below 2.5 GeV/c, χ^2/n for the fit (6-7) with $P_0 = 4.5$ GeV/c is equal to 2.46 at 466 data points. The results are shown by the dash- dotted lines. The dashed lines are the results of the fit for initial momenta between 2 and 2.5 ($P_0 = 2.25$ GeV/c), 2.5 and 3.5 ($P_0 = 3.0$ GeV/c), 3.5 and 5.2 ($P_0 = 4.5$ GeV/c), 5.2 and 6.0 GeV/c ($P_0 = 6.0$ GeV/c), respectively. The optimum values for the 14-parameter fits (6-7) of the *pp*- elastic scattering data are presented in Table 2.

All the fits performed within a wide range of the initial momenta give approximately the same behaviour of the analyzing power. However, the fits for "narrow" ranges, except the range between 5.2 and 6.0 GeV/c, show a different behaviour. The fit gives systematically lower values of analyzing power at $\theta \geq 10°$ nearby 2.25 GeV/c, predicts a larger value of A at 3.0 GeV/c and demonstrates a shift of the maximum value of the analyzing power at 4.5 GeV/c.

The behaviour of the analyzing power at large angles (large $|t|$) also differs significantly for two types of fit. As the fit taken in the form of (4-5) predicts an increase of the analyzing power at large $|t|$, parametrization (6-7) gives a smooth decrease of the analyzing power at momenta lower than 3.5 GeV/c and an oscillating behaviour at larger momenta.

Finally, one can conclude that both fits reasonably reproduce the data. However, the systematic error of the fitting procedure can be roughly estimated as $\sim 10\%$. The choice of parametrization depends on the physical goal and the angular and momentum region.

4 Parametrization of *np*- elastic scattering analyzing power

The same parametrizations were done for the *np*- elastic scattering data obtained at 2, 3, 4 and 6 GeV/c [13]. The results of the fit taken in the form of (4-5) are shown in Fig.4. The solid lines represent the results of the fit obtained over a momentum domain of 2-6 GeV/c. This fit includes 56 data points and gives $\chi^2/n = 1.76$. The dashed lines are the results of the fit performed at fixed initial momenta. One can see that the results of both fits give approximately the same behaviour although fixed momentum fits provide a better agreement with the data. The optimum values for the 8-parameter fit (4-5) of the *np*- elastic scattering data are presented in Table 3.

The same data [13] were parametrized using the function depending on initial momentum and scattering angle (6-7). The results of the fit are presented in Fig.5. This fit gave $\chi^2/n = 1.44$. The optimum values for the 14-parameter fit (6-7) are presented in Table 4.

5 Analyzing powers at 8° in lab.

From the practical point of view, it is useful to have the data parametrization at a fixed angle in the lab. For instance, the data on *pp*- analyzing power at 11.6°, 13.0° and 13.9° in the lab. were fitted as a linear function of kinetic energy, T_{kin}, between 1.6 and 3.6 GeV [2]:

$$A(11.6° lab) = 0.50745 - 0.10768 \cdot T_{kin} \tag{8}$$
$$A(13.0° lab) = 0.53757 - 0.12957 \cdot T_{kin} \tag{9}$$
$$A(13.9° lab) = 0.62310 - 0.17978 \cdot T_{kin} \tag{10}$$

However, the analyzing power as a function of scattering angle (at $\theta \geq 8°$) decreases with increasing initial energy, and, so the use of elastic scattering at smaller angles is more convenient for polarimetry purposes at high energies. The analyzing powers of *pp*- and *np*- scattering at 8° in the lab. (see ref.[3]) were parametrized as a linear function of kinetic energy, T_{kin}:

$$A_{pp}(8° lab) = 0.3874 - 0.05849 \cdot T_{kin} \tag{11}$$
$$A_{np}(8° lab) = 0.2549 - 0.05318 \cdot T_{kin} \tag{12}$$

with $\chi^2/n = 1.97$ and 0.97, respectively.

The quadratic fit of the *pp*- analyzing power gives:

$$A_{pp}(8° lab) = 0.51640 - 0.13000 \cdot T_{kin} + 0.009056 \cdot T_{kin}^2 \tag{13}$$

with $\chi^2/n = 1.74$

The data on the analyzing power of *pp*- and *np*- elastic scattering at 8° in the lab. are shown in Figs.6 and 7, respectively. The solid lines are the results of linear fits (11) and (12). The dashed lines represent the phase shift analysis solution [4]. The dotted line in Fig.6 is the result of quadratic fit (13). The point at $T_{kin} = 635$ MeV in Fig.7 is taken from ref.[30]. As the *pp-* data have a positive sign over the range of the fit, the *np-* data demonstrate the crossing of zero at $T_{kin} \sim 4.8$ GeV. One can also see that the quadratic fit does not improve significantly the description of the data due to large errors of *pp-* data at 8^o.

The systematic error due to different parametrizations of the data at 8^o can be estimated for the *pp-* and *np-* analyzing powers from Figs.8 and 9, respectively. The solid and dashed lines in these figures represent the results of the linear and quadratic fits at 8^o, respectively. The dashed and dash-dotted lines are parametrizations (4-5) and (6-7) taken at a fixed angle of 8^o in lab., respectively. For instance, the systematic error of the analyzing power of *pp-* elastic scattering at 8^o and 3.66 GeV is $\sim 9\%$. The recommended values of the *pp-* and *np-* analyzing powers at 8^o are given in Table 5.

The performance of a polarimeter is expressed in terms of the figure of merit, $\mathcal{F}$. The $\mathcal{F}$ is the function of efficiency ϵ and analyzing power A. It is defined as

$$\mathcal{F}^2 = \int \epsilon A^2 d\Omega, \tag{14}$$

where Ω is the solid angle, and integration is over the angular domain of the polarimeter. The figure of merit allows one to evaluate the counting rate N_{inc} necessary to obtain the desired precision of polarization ΔP:

$$\Delta P \approx \frac{\sqrt{2}}{\mathcal{F}\sqrt{N_{inc}}} \tag{15}$$

Since the cross section of *pp-* elastic scattering decreases fastly as a function of scattering angle, the polarimeter figure of merit $\mathcal{F}$ also decreases versus angle. Therefore, polarimetry at smaller angles is more convenient if the analyzing power varies smoothly at a fixed energy. The analyzing power A and the figure of merit $\mathcal{F}$ as a function of initial energy for different scattering angles are plotted in Figs.10a and 10b, respectively. The solid, dashed and dotted lines are obtained using the linear parametrizations of the analyzing power at 8^o, 11.6^o and 13.0^o, respectively (see expressions (11), (8) and (9)). The dash-dotted lines are obtained using the quadratic parametrization of the analyzing power at 13.9^o in the lab.[2]:

$$A(13.9^o lab) = 0.79849 - 0.33118 \cdot T_{kin} + 0.032327 \cdot T_{kin}^2 \tag{16}$$

The figure of merit of the polarimeter was calculated for a 2 *cm* polyethylene target along the beam direction using the parametrization of the *pp-* elastic scattering cross section from [31]. One can see a strong variation of the figure of merit versus initial energy. It drops by a factor of ~ 2 between 2.2 and 3.66 GeV and ~ 10 between 2.2 and 5.135 GeV at a scattering angle of 8^o. The figure of merit at 2.2 GeV and 8^o is approximately as twice as large as that at 11.6^o although the analyzing power has approximately the same value at both angles. This ratio increases with increasing of energy, and it is approximately equal to 3 at 3.66 GeV. The use of this polarimeter in such a configuration provides the error bar $\Delta P = 0.02$ during the measurements of the deuteron beam polarization with a typical intensity of $\sim 2 \cdot 10^9$ particles per burst for ~ 1 hour at the highest available energy of the Synchrophasotron (3.66 GeV/c per nucleon). For instance, the vector admixture of the beam polarization measured by the polarimeter [5] with a 5 *mm* CH_2 target during the experiment on the tensor analyzing power A_{yy} in deuteron inclusive breakup at 9 GeV/c [9, 10] (full symbols in Fig.1) was $p_z^+ = 0.234 \pm 0.032$ and $p_z^- = 0.250 \pm 0.032$ for the " + " and " − " beam polarization states [1], respectively. Such error bars were obtained for ~ 3 hours of measurements.

However, the *pp-* elastic scattering at 8^o cannot be efficiently used for beam polarization measurements at larger momenta because of a small figure of merit. The analyzing power and the figure of merit of the polarimeter at fixed 4-momenta $-t = 0.15$, 0.25 and 0.4 $(GeV/c)^2$ are shown in Fig.11 by the dashed, dash-dotted and dotted lines, respectively. The curves are obtained using the parametrization of the analyzing power (4-5) with the parameters presented in Table 1. The solid lines represent A and $\mathcal{F}$ at 8^o in the lab. One can see that it is necessary to use *pp-* scattering at angles smaller than 8^o (between 4^o and 6^o) for polarimetry purposes at energies higher than the maximum energy of the Synchrophasotron. However, good parameters of the beam on the target are required in this case. Such beam parameters will be accessible at the new superconducting accelerator Nuclotron at LHE.

6 Conclusions

The results of this work are the following:

- The parametrizations of the *pp-* and *np-* elastic scattering analyzing powers as a function of incident momentum and 4-momentum, incident momentum and scattering angle are obtained. Such parametrizations are useful to evaluate the counting rates for experiments calling for polarimeters.
- It is shown that the vector polarization of the deuteron beam can be obtained for the energy domain of Synchrophasotron (up to 3.66 GeV/nucleon) from the left-right asymmetry measurements of *pp-* quasielastic scattering at 8^o with a systematic error of $\sim 6\%$ and $\sim 9\%$ at 2.2 and 3.66 GeV/nucleon, respectively.
- The experimental results show that the use of a relatively thick (2 *cm* along the beam direction) CH_2 target and scattering at 8^o and 3.66 GeV/nucleon provides a statistical error of 0.02 per hour of the beam time under typical operating conditions. At higher energies, scattering at angles smaller than 8^o is more convenient for beam polarimetry.

[1]The beam polarization values were obtained taking into account the carbon content of the CH_2 target.

Table 1. Optimum values for the 8-parameter fit [1] of the *pp*- elastic scattering analyzing power for incident momenta between 2.0 and 6.0 GeV/c and $|t| \leq 1.5$ $(\mathrm{GeV/c})^2$.

Momentum range, GeV/c	D	E	F	G	H	J	K	L	χ^2/n
2.0-6.0	2.26± 0.16	0.002± 0.058	0.011± 0.007	1.29± 0.05	0.281± 0.066	0.0131± 0.0249	0.175± 0.036	0.496± 0.026	2.95
2.0-5.2	3.54± 0.30	−0.492± 0.119	0.083± 0.020	1.69± 0.07	−0.266± 0.104	0.158± 0.053	0.431± 0.061	0.248± 0.053	3.41
2.0-2.5	2.1± 0.2	0.092± 0.016	0.00524± 0.00398	1.38± 0.13	−0.386± 0.017	0.89± 0.19	−0.0911± 0.254	0.978± 0.318	3.03
2.5-3.5	−57.2± 0.1	24.0± 0.04	−4.06± 0.01	−0.273± 0.031	4.56± 0.03	−2.65± 0.03	1.23± 0.03	−0.521± 0.026	4.18
3.5-5.2	−3.19± 0.18	1.70± 0.05	−0.177± 0.009	0.622± 0.049	1.25± 0.04	−0.367± 0.024	0.508± 0.050	0.200± 0.034	1.86
5.2-6.0	23.1± 0.2	0.336± 0.027	−0.633± 0.005	1.35± 0.03	−0.366± 0.019	0.372± 0.011	0.757± 0.031	0.203± 0.018	1.28

Table 2. Optimum values for the 14-parameter fit [29] of the *pp*- elastic scattering analyzing power for incident momenta between 2.0 and 6.0 GeV/c and $\theta \leq 30°$.

Momentum range, GeV/c	P_0		0	1	2	χ^2/n
2.0-6.0	4.0	a	28.3 ± 1.1	−4.97 ± 0.29	0.0512 ± 0.217	2.94
		b	6.15 ± 0.05	0.145 ± 0.016	−0.091 ± 0.014	
		c	2.70 ± 0.025	4270 ± 952	−6300 ± 1010	
		d	4520 ± 779	11.4 ± 0.23	−0.901 ± 0.047	
		r	0.583 ± 0.037			
		s	17.3 ± 0.3			
2.0-5.2	4.0	a	74.7 ± 12.6	−28.1 ± 4.93	−4.97 ± 1.61	3.17
		b	7.16 ± 0.20	−0.335 ± 0.078	−0.298 ± 0.038	
		c	3.37 ± 0.11	42.5 ± 13.4	−85.2 ± 21.5	
		d	149 ± 29	6.85 ± 0.25	−0.574 ± 0.064	
		r	1.08 ± 0.10			
		s	11.3 ± 0.35			
2.0-2.5	2.25	a	130 ± 11.8	−98.8 ± 17.8	−2850 ± 310	4.78
		b	17.6 ± 1.4	0.522 ± 0.727	−160 ± 14.8	
		c	2.77 ± 0.18	126 ± 13.3	−69.8 ± 18.0	
		d	−86.8 ± 75	7.44 ± 0.17	−1.32 ± 0.32	
		r	−17.2 ± 3.2			
		s	3.38 ± 0.05			
2.5-3.5	3.0	a	10.7 ± 2.5	−0.140 ± 9.97	424 ± 21.7	2.40
		b	5.89 ± 0.03	4.62 ± 0.32	11.7 ± 0.4	
		c	2.68 ± 0.05	0.954 ± 0.126	2.60 ± 0.44	
		d	−20.8 ± 2.33	1.96 ± 0.10	−4.45 ± 0.40	
		r	−0.997 ± 0.768			
		s	0.906 ± 0.079			
3.5-5.2	4.0	a	66.0 ± 12.2	38.8 ± 9.46	186 ± 31.4	1.43
		b	6.91 ± 0.22	0.801 ± 0.094	2.84 ± 0.26	
		c	3.61 ± 0.11	95.1 ± 9.5	119 ± 28.4	
		d	568 ± 141	7.80 ± 0.16	0.221 ± 0.071	
		r	1.66 ± 0.29			
		s	12.8 ± 0.4			
5.2-6.0	6.0	a	3.95 ± 0.37	2.10 ± 6.95	−55.2 ± 80.8	1.57
		b	4.31 ± 0.11	4.75 ± 2.65	−53.9 ± 30.8	
		c	1.83 ± 0.05	13400 ± 1690	−2900000 ± 330000	
		d	11000000 ± 1200000	12.50 ± 0.14	−7400 ± 891	
		r	85900 ± 10300			
		s	18.50 ± 0.26			
2.5-6.0	4.5	a	11.2 ± 0.65	−2.40 ± 0.18	1.11 ± 0.19	2.46
		b	5.08 ± 0.06	0.085 ± 0.013	0.104 ± 0.014	
		c	2.32 ± 0.03	180 ± 5	−192 ± 17.1	
		d	396 ± 50	8.78 ± 0.10	−0.360 ± 0.015	
		r	0.536 ± 0.031			
		s	14.5 ± 0.2			

Table 3. Optimum values for the 8-parameter fit [1] of the *np*- elastic scattering analyzing power for incident momenta between 2.0 and 6.0 GeV/c [13].

Momentum range, GeV/c	D	E	F	G	H	J	K	L	χ^2/n
2.0-6.0	3.74± 0.35	−0.687± 0.119	0.0533± 0.015	1.87± 0.27	−0.658± 0.308	0.485± 0.16	0.213± 0.50	0.387± 0.397	1.76
2.0	2.29± 0.38	0.0062± 0.0944	−0.0411± 0.0708	2.05± 0.18	−0.223± 0.264	0.386± 0.381	0.821± 0.346	0.502± 0.500	2.73
3.0	1.97± 0.34	−0.0595± 0.0851	−0.0536± 0.038	1.86± 0.25	−0.444± 0.226	0.115± 0.206	0.363± 0.328	0.0103± 0.298	1.62
4.0	1.87± 0.40	−0.0558± 0.079	−0.0636± 0.025	1.72± 0.45	−0.533± 0.323	0.0677± 0.233	0.0239± 0.587	−0.174± 0.424	1.64
6.0	1.80± 1.11	−0.0323± 0.158	−0.0182± 0.0308	2.19± 0.59	−0.229± 0.328	0.267± 0.183	0.729± 0.594	0.327± 0.332	1.19

Table 4. Optimum values for the 14-parameter fit [29] of the *np*- elastic scattering analyzing power for incident momenta between 2.0 and 6.0 GeV/c [13].

Momentum range, GeV/c	P_0		0	1	2	χ^2/n
2.0-6.0	4.0	a	8990 ± 2.9	-5660 ± 1.5	571 ± 0.7	1.44
		b	12.1 ± 0.15	-2.49 ± 0.15	-0.696 ± 0.060	
		c	-4.75 ± 0.043	-3.75 ± 0.02	3.18 ± 0.01	
		d	4.33 ± 0.22	-1.36 ± 0.04	-0.386 ± 0.031	
		r	6.88 ± 0.053			
		s	2.71 ± 0.11			

Table 5. Analyzing powers of *pp*- and *np*- elastic scattering at 8° in the lab. versus incident momentum per nucleon.

Momentum GeV/c	$A_{pp} \pm dA_{pp}$	$A_{np} \pm dA_{np}$
3.0	0.260 ± 0.015	0.142 ± 0.010
4.5	0.168 ± 0.015	0.065 ± 0.010
6.0	0.087 ± 0.005	-0.021 ± 0.007

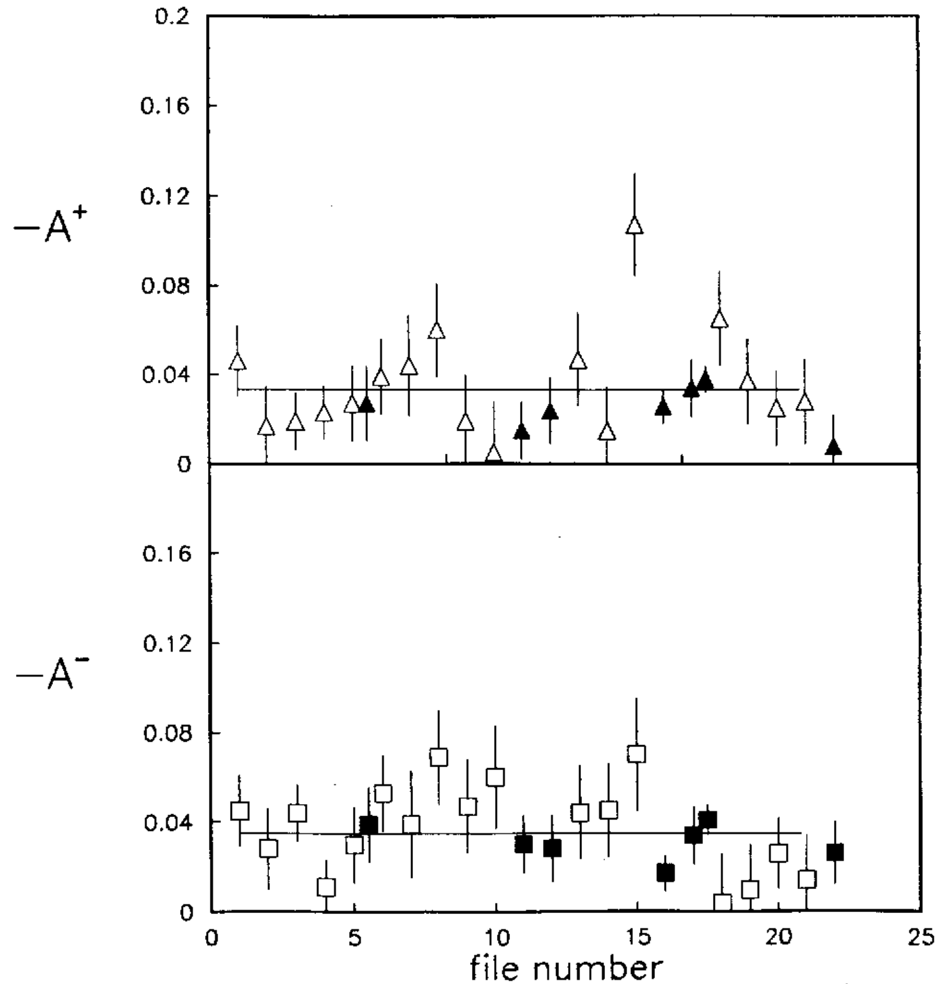

Fig.1. Asymmetries $A^{\pm}$ from the polarimeter [5]. The open and full symbols are the values of asymmetries $A^{\pm}$ obtained during the control measurements of polarization and data taking, respectively [10].

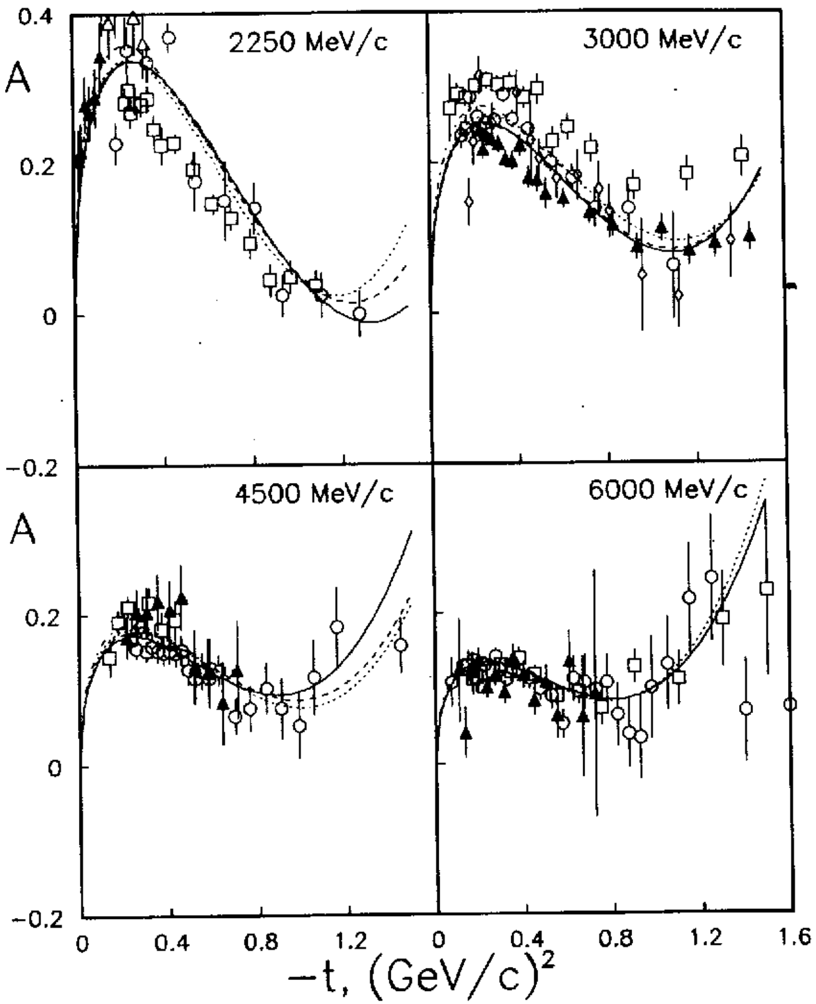

Fig.2. The 8-parameter fit (4-5) of the analyzing power of *pp*- elastic scattering. The solid and dashed lines represent the results of the fit over an initial momentum range of 2-6; 2-5.2, respectively, for 2.25, 3, 4.5 and 6 GeV/c. The dotted lines are the results of the fit for momentum domains of 2-2.5, 2.5-3.5, 3.5-5.2 and 5.2-6 GeV/c, respectively. The dash-dotted lines are the results of parametrization from ref.[1]. The symbols are the data from ref.[3].

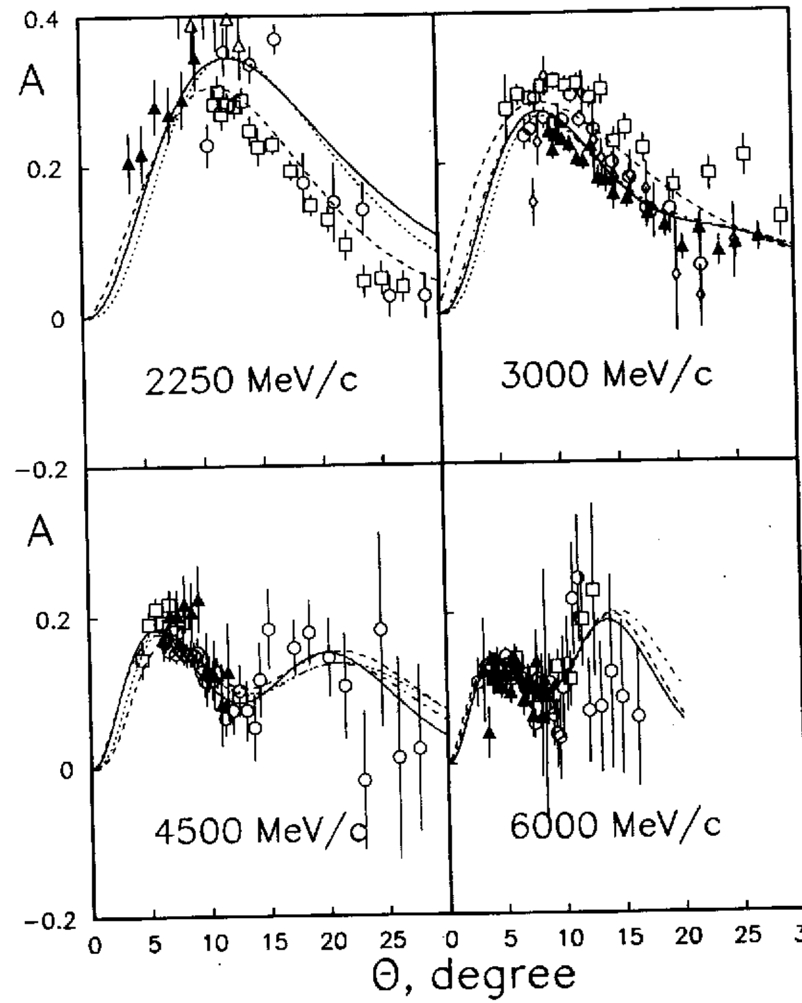

Fig.3. The 14-parameter fit (6-7) of the analyzing power of *pp*- elastic scattering. The lines are explained in the text. The symbols are from ref.[3] and the same as in Fig.2.

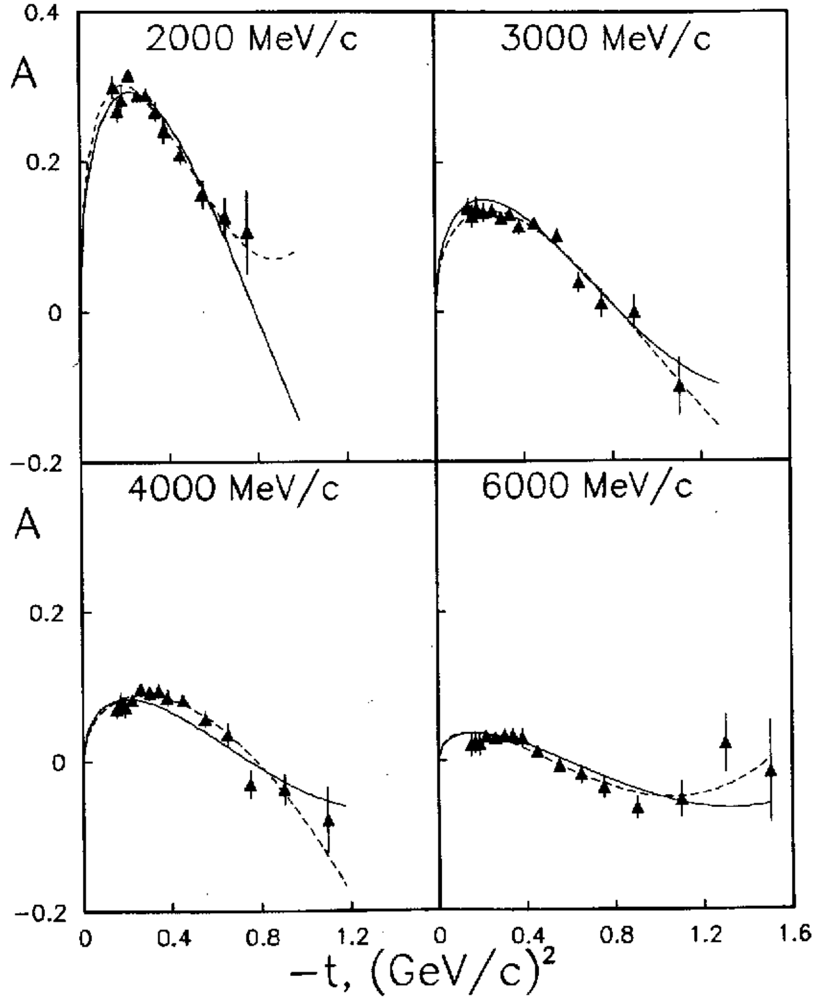

Fig.4. The results of the fit (4-5) for the np- elastic scattering data [13]. The solid lines represent the results of the fit obtained over a momentum domain of 2-6 GeV/c. The dashed lines are the results of the fit performed at fixed initial momenta.

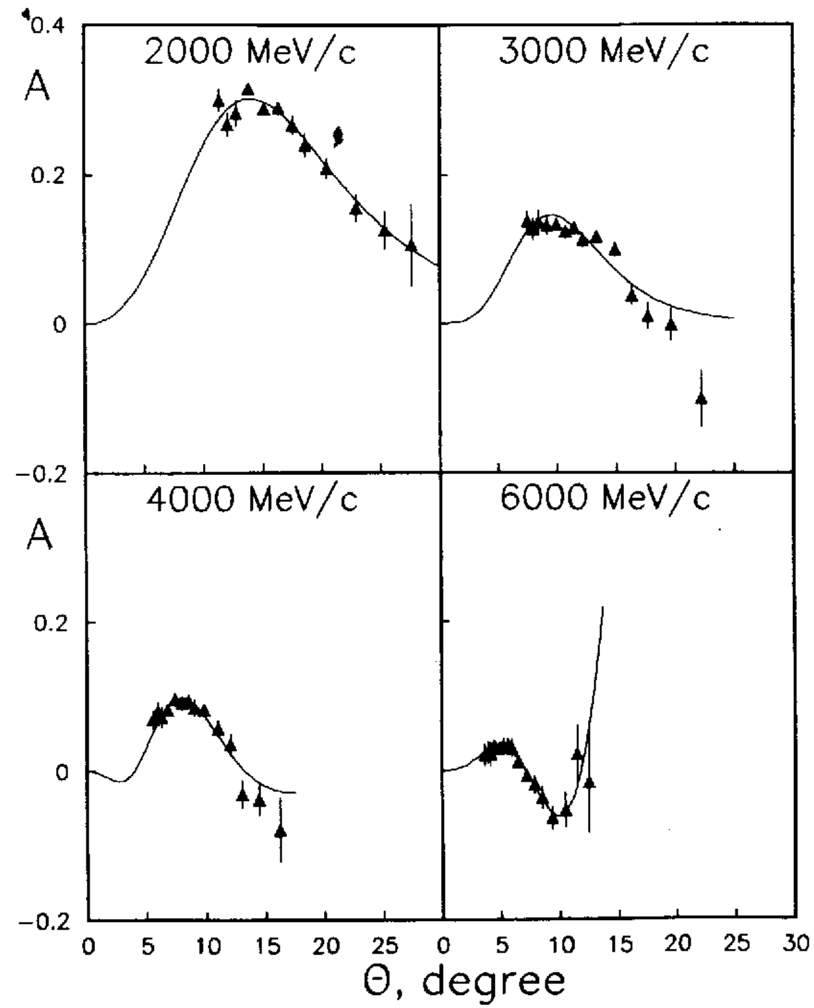

Fig.5. The results of the fit (6-7) for the np- elastic scattering data [13]. The solid lines represent the results of the fit obtained over a momentum domain of 2-6 GeV/c.

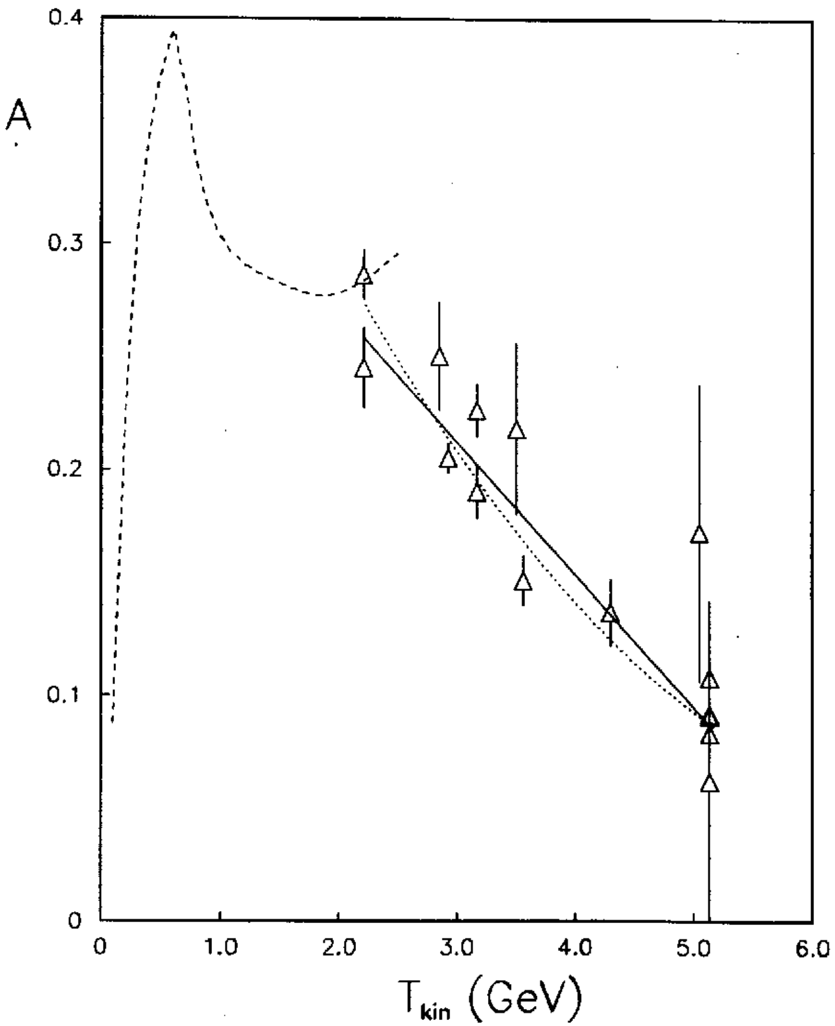

Fig.6. The data on the analyzing power of *pp*- elastic scattering at 8^o in the lab. The solid and dotted lines are the results of the linear and quadratic fits, respectively. The dashed line represents the phase shift analysis solution [4].

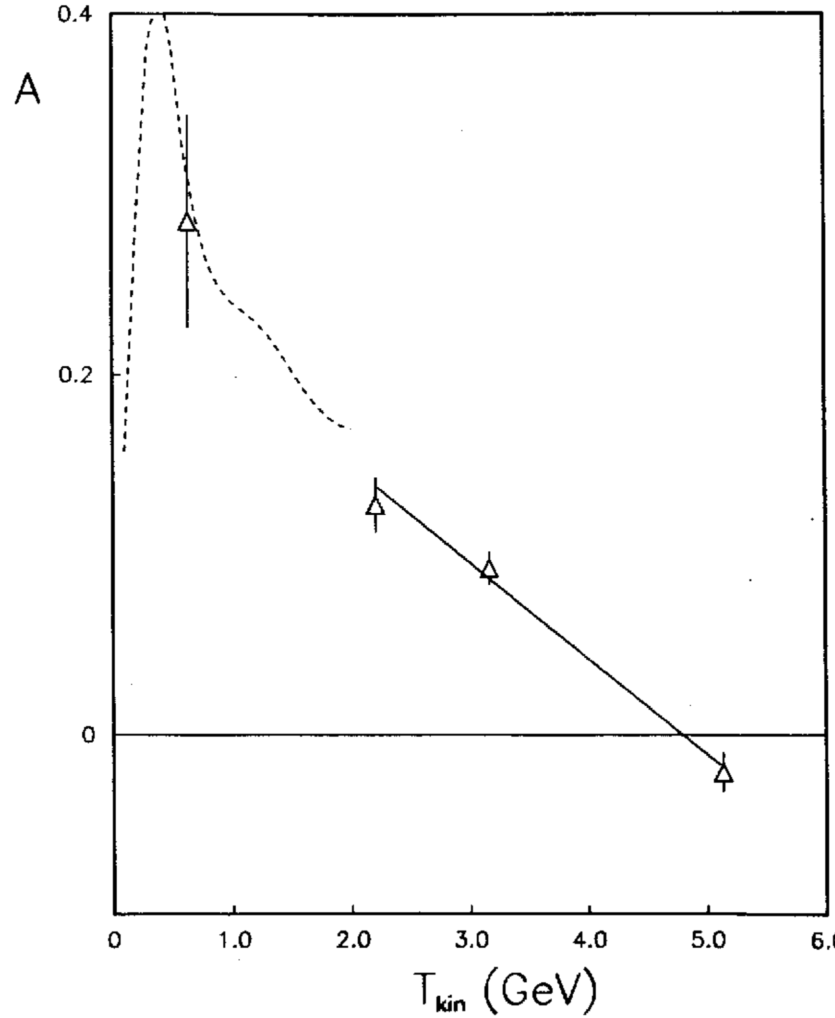

Fig.7. The data on the analyzing power of *np*- elastic scattering at 8^o in the lab. The solid line is the result of the linear fit. The dashed lines represent the phase shift analysis solution [4]. The point at T_{kin} = 635 MeV is taken from ref.[30].

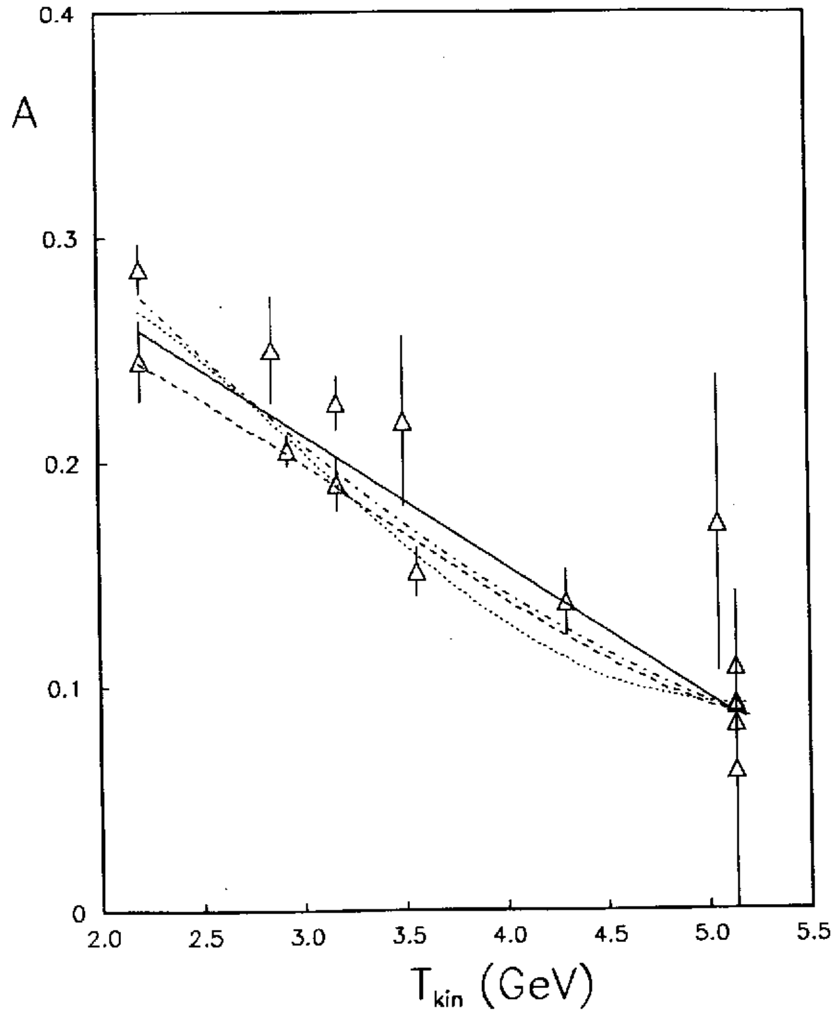

Fig.8. The solid and dashed lines represent the results of a linear and quadratic dependence of the *pp*- analyzing power at 8° on kinetic energy, respectively. The dashed and dash-dotted lines are parametrizations (4-5) and (6-7) taken at a fixed angle of 8° in the lab., respectively.

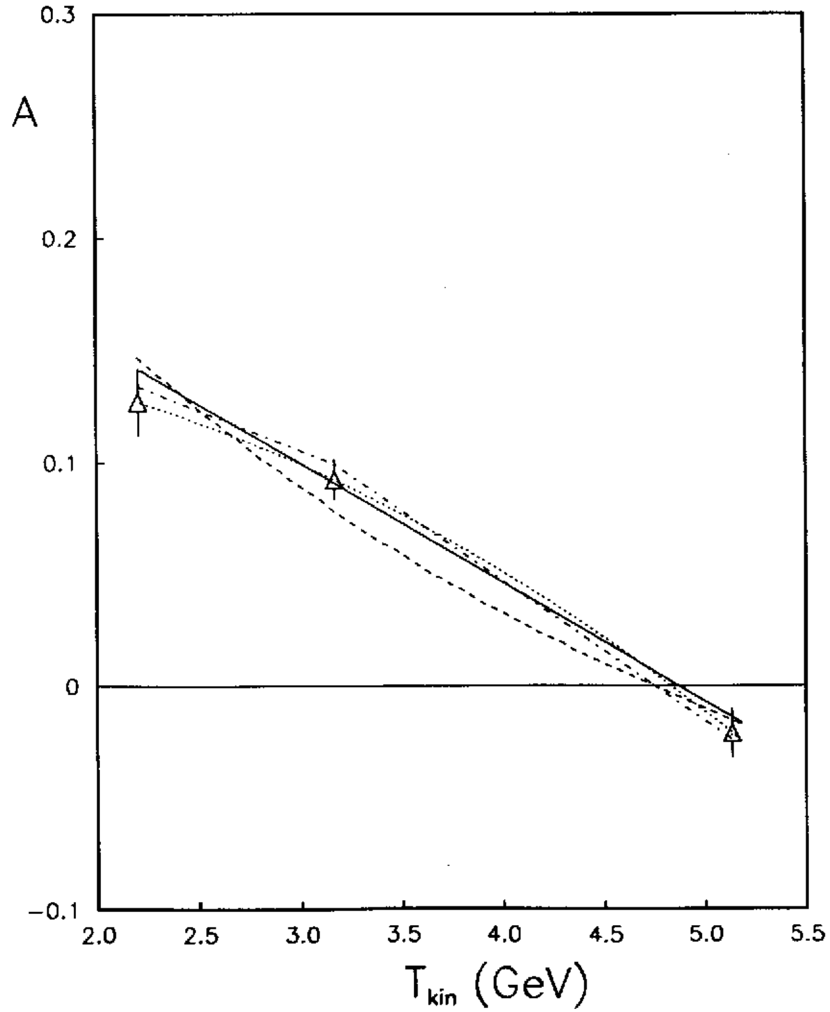

Fig.9. The solid and dashed lines represent the results of a linear and quadratic dependence of the *np*- analyzing power at 8° on kinetic energy, respectively. The dashed and dash-dotted lines are parametrizations (4-5) and (6-7) taken at a fixed angle of 8° in the lab., respectively.

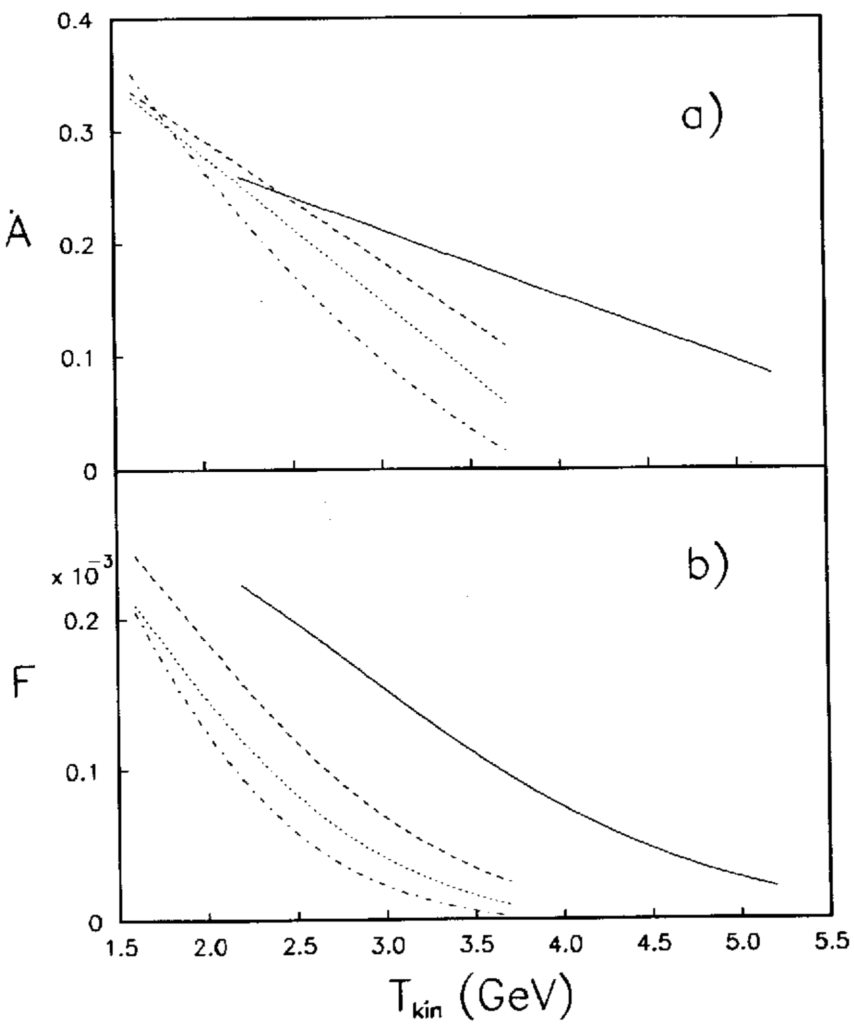

Fig.10. a) The analyzing power A and b) the figure of merit $\mathcal{F}$ as a function of initial energy at different scattering angles. The solid, dashed, dotted and dash-dotted lines are obtained at angles of 8°, 11.6°, 13.0° and 13.9°, respectively.

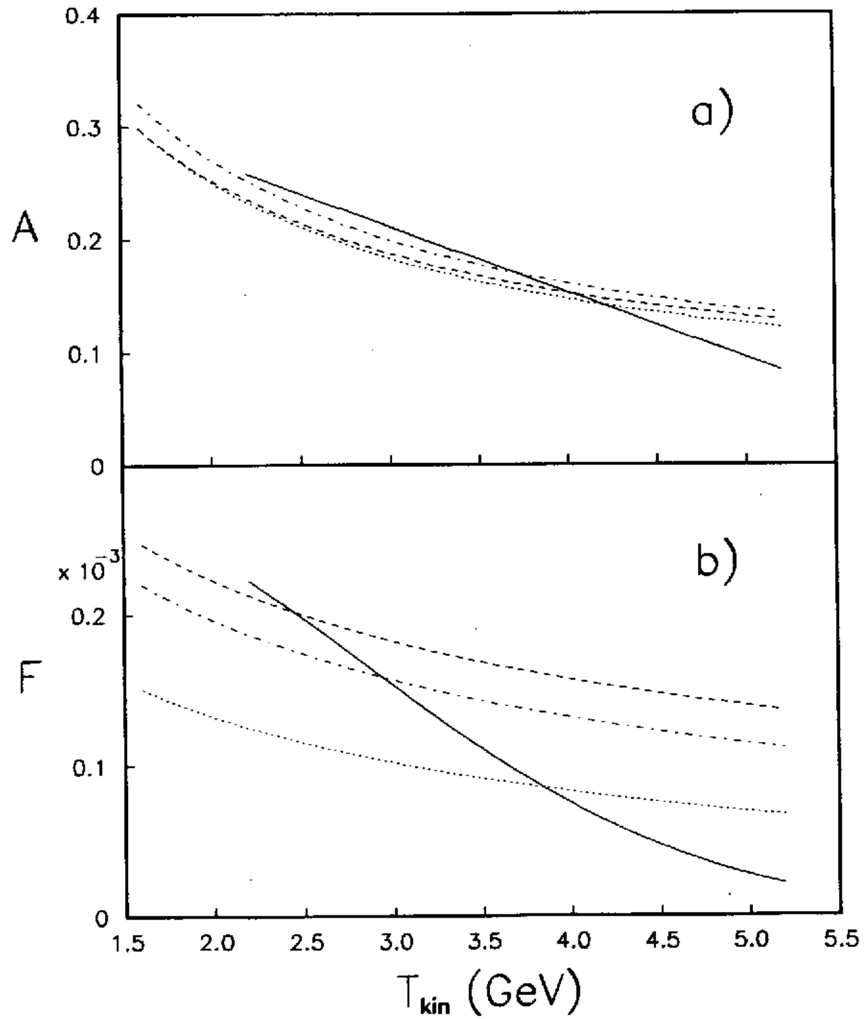

Fig.11. a) The analyzing power A and b) the figure of merit $\mathcal{F}$ as a function of initial energy taken at fixed 4-momenta. The dashed, dash-dotted and dotted lines are obtained at $-t = 0.15$, 0.25 and 0.4 $(GeV/c)^2$, respectively. The solid lines are the analyzing power and the figure of merit at a fixed scattering angle of 8° in the lab.

Acknowledgements

The author thanks Professor L.S. Azhgirey, G.D. Stoletov and V.N. Zhmyrov for fruitful discussions.

References

[1] H. Spinka et al., Nucl.Instr. and Meth. 211 (1983) 239.

[2] Ch. Allgower et al., Preprint LNS/Ph/97-11 (1997) Gif-sur-Yvette.

[3] J. Bystricky and F. Lehar, Nucleon-nucleon scattering data, Fachinformationszentrum Karlsruhe, 11-1 (1978) and 11-2 (1981).

[4] R.A. Arndt et al., Phys.Rev. C56 (1997) 3005.

[5] L.S. Azhgirey et al., PTE 1 (1997) 51.

[6] G. Olhsen, Rep.Prog. 35 (1972) 717.

[7] N.G. Anishchenko et al., Proc. 5-th Int.Symp. on High Energy Spin Physics (Brookhaven, 1982), AIP Conf.Proc. 95 (N.Y.1983) 445.

[8] B.P. Adiasevich et al., Z.Phys. C71 (1996) 65.

[9] S.V. Afanasiev et al., Phys.Lett. B434 (1998) 21.

[10] S.V. Afanasiev et al., JINR Rapid Comm. 2[88]-98 (1998) 5.

[11] V.G. Ableev et al., Nucl.Instr. and Meth.A306 (1991) 73.

[12] D.Miller et al., Phys.Rev.D16 (1977) 2016.

[13] R. Diebold et al., Phys.Rev.Lett. 35 (1975) 632.

[14] H.A. Neal, M.J. Longo, Phys.Rev. 161 (1967) 1374.

[15] M.G. Albrow et al., Nucl.Phys. B23 (1970) 445.

[16] V.V. Zhurkin et al., Yad.Fiz.28 (1978) 1280;
Soviet J.Nucl.Phys. (English transl.) 28 (1978) 660.

[17] P. Grannis et al., Phys.Rev. 148 (1966) 1280.

[18] J.H. Parry et al., Phys.Rev. D8 (1973) 45.

[19] J. Deregel et al., Nucl.Phys. B103 (1976) 269.

[20] G.W. Abshire et al., Phys.Rev.Lett. 32 (1974) 1261.

[21] M. Borghini et al., Phys.Lett. B24 (1966) 77.

[22] M. Borghini et al., Phys.Lett. B31 (1970) 405.

[23] J.R. O'Fallon et al., Phys.Rev.Lett. 32 (1974) 77.

[24] R.C. Fernow et al., Phys.Lett. B52 (1974) 243.

[25] D.R. Rust et al., Phys.Lett. B58 (1975) 114.

[26] R.D. Klem et al., Phys.Rev. D15 (1977) 602.

[27] L.G. Ratner et al., Phys.Rev. D15 (1977) 604.

[28] M. Borghini et al., Phys.Rev. D17 (1978) 24.

[29] N.E. Cheung et al., Nucl.Instr. and Meth.A363 (1995) 561.

[30] V.P. Dzhelepov et al., Proc. of the XIIth Int. Conf. on High Energy Physics, Dubna (1964) 11.

[31] L.S. Azhgirey, S.V. Razin and N.P. Yudin, Yad.Fiz. 46 (1987) 1657;
Soviet J.Nucl.Phys. (English transl.) 46 (1987) 988.

**Received by Publishing Department
on April 22, 1999.**